

Physics laboratory -LM, A.A. 2021/22

Group: 5

Cohort: 1

Experience date: 18-22-23/11/2021

Delivery date: 3-12-2021

Giovanni Celotto 2052372 giovanni.celotto@studenti.unipd.it

Andrea Pompermaier 2053046 andrea.pompermaier@studenti.unipd.it

Massimo Colombo 2056104 massimo.colombo@studenti.unipd.it

Cristian Tibambre 2054971 cristiandavid.tibambreheredia@studenti.unipd.it

Measurement of Environmental Radiation

1 Introduction

The environment in which we live is permeated by different radioactive sources, originated through different types of processes:

- Primordial radionuclides, such as ^{40}K and the products of ^{238}U decay chain, have been produced billions of years ago during the nucleosynthesis process and thanks to their long half-life they can still be observed nowadays. They are typically contained inside particular types of rocks.
- Radioactive nuclei such as ^{14}C or ^3H are produced from the interaction of high-energy cosmic rays with the higher layers of the atmosphere. In particular, ^{14}C can be absorbed by plants and then enters the life cycle of living beings.
- Artificial sources (e.g. nuclear power plants, nuclear wastes, or weapons) can take on great importance to environmental pollution. For example, a great part of the radioactive materials (such as ^{137}Cs) released during the explosion of the nuclear reactor of Chernobyl (1986) is still present in our environment.

One of the most dangerous environmental radionuclides is the ^{222}Rn : a noble gas belonging to the ^{238}U decay chain. It has a half-life of 3.8 days and it α -decays to ^{218}Po . It is an odorless and colorless gas that typically accumulates on the lower layers of air, especially in rooms with low ventilation located near the ground floor.

2 Objectives

The main purpose of this experience is the measurement of environmental radiation using NaI(Tl) and HPGe detectors, and in particular of:

- Optimization of the resolution of detectors by adjusting the parameters of trapezoidal filter.
- Measurement of the intrinsic efficiency of the two detectors.
- Measurement of the activity of some known samples.
- Measurement of the activity of Radon which is present in the cellar of the Polo Didattico.

3 Experimental setup

The experimental setup for this experiment consists of:

- Some known radioactive sources:
 - ^{241}Am (Nº 148) with activity $A_{Am} = 419kBq$;
 - ^{60}Co (Nº 143) with activity $A_{Co} = 195kBq$;
 - ^{152}Eu (Nº 87) with activity $A_{Eu} = 84kBq$;
 - ^{226}Ra (Nº 105) with activity $A_{Ra} = 0.524kBq = 14.2nCi$;
- Some organic and inorganic samples:
 - 15g of mushrooms picked in 1986 after the Chernobyl disaster;
 - 1870g of zirconium oxide;
 - 500g of water (ENEA);
 - 490g of porphyry;
 - 30g of Autunite;
- Two sealed cylindrical canisters of activated charcoal: one is opened and exposed to the air, instead the other is left close (background canister). (diameter 10cm and height 3cm)
- A calibration canister that contains ^{226}Ra . (diameter 10cm and height 3cm)
- There are two γ -detectors positioned inside a cockpit of lead and copper (used to shield low-background):
 - A cylindrical HPGe detector (ORTEC GMX) with endcap diameter $(7.0 \pm 0.1)\text{cm}$ (nominal detection area $\sim 1200\text{mm}^2$);
 - A cylindrical NaI(Tl) scintillator (SCIONIX HOLLAND SFQ658) with diameter $(8.0 \pm 0.1)\text{cm}$ (effective detection area $\sim 4420\text{mm}^2$) connected to photomultipliers (SCIONIX HOLLAND SVE984).
- A Caen DT5780 digitizer with two channels, 100 MS/s 14-bit.
- An oscilloscope Textronix TBS 1102B-EDU, 100MHz 2 GS/s.
- A computer which uses Verdi acquisition system.
- A weight scale.

4 Calibration of the detectors

The first part of the experiment consists in optimizing the detectors resolution, by modifying the characteristic parameters of the trapezoidal filter, and then calibrating each detector by acquiring spectra of known sources.

After placing the detectors we connected them to the power supply and before doing the measurements we waited for the tension to reach the optimal values (+700V for NaI(Tl) and -2000V for HPGe). In order to verify the correct operation of the detectors, we inserted in the cockpit a ^{60}Co source and we connected their outputs directly to the oscilloscope. This procedure was useful to have an idea of the characteristics of the pre-amplified signal of a known transition (we selected the 1332keV peak) by measuring:

- The maximum amplitude: $\sim 110mV$ for HPGe and $\sim 230mV$ for NaI(Tl);
- The linear fall time width: $\sim 1.5\mu s$ for HPGe and $\sim 2\mu s$ for NaI(Tl);
- The exponential rising time width: $\sim 52\mu s$ for HPGe and $\sim 70\mu s$ for NaI(Tl);
- The noise level which is around $20mV$ for both detectors.

Then we connected the outputs of the detectors to the digitizer (ch0 for NaI(Tl) and ch1 for HPGe) and we proceeded by adjusting the trapezoidal filter parameters in order to optimize the resolution of the 1332keV peak for each detector.

4.1 Trapezoidal filter optimization

A trapezoidal filter is necessary to properly select the events that must be analyzed by the digitizer. A correct selection of the events is necessary to have an optimal resolution and to study in detail the isotopes that are present in a sample. The parameters which affect the trapezoidal filter are:

- Trigger threshold: it has been adjusted in order to reduce the electronic noise, which appears at low energies, without cutting away the 59keV peak of ^{241}Am from the spectrum.
- Decay time: it represents the exponential decay time of the pre-amplified signal. It has a value that typically belongs to the range $[50\mu\text{s}, 100\mu\text{s}]$.
- Trapezoidal rise time: it is the temporal width of the rising pre-amplified signal. It has a value that typically belongs to the range $[0.5\mu\text{s}, 5\mu\text{s}]$.
- Trapezoidal flat top: it's a value corresponding to the small flat range on the top of the trapezoid produced by the pre-amplified signal. It typically belongs to the range $[0.1\mu\text{s}, 1\mu\text{s}]$.
- Trapezoidal re-scaling: this parameter can, if necessary, re-scale the spectrum to better visualize it.

The threshold and the re-scaling parameters can be adjusted in a second moment (we initially put default values), since to optimize the peak resolution it's necessary to first adjust the decay time, the rise time and the flat top. They affect at the same time the shape of the peak so we have adopted a strategy to find them in order to have the best possible resolution. We started by setting as decay time and rise time the values that we obtained from the measurement with the oscilloscope and a reliable value for the flat top (e.g. $0.5\mu\text{s}$) (these temporal values are expressed in arbitrary units of the digitizer: $1\text{a.u.} = 0.01\mu\text{s}$). The decay time has been adjusted to make the flat top to be flat and then it has been fixed. Then we scanned, for different values of the rising time, the resolution of the 1332keV peak of ^{60}Co until we have reached a minimum and we fixed that value. We proceed in the same way also for the flat top parameter. This method allows finding a local minimum of the peak resolution. To have a global minimum it would be necessary to compare the resolution by making a three-dimensional scan: this rigorous procedure it's long and not necessary for our scope. The parameters obtained from the optimization procedure have been manually adjusted in order to reproduce a good gaussian shape. The final parameters obtained for each detector (in Tab. 1) have been saved in the Verdi configuration file.

Detector	Threshold [a.u.]	Decay time [a.u.]	Rise time [a.u.]	Flat top [a.u.]	Re-scaling	R [%]
NaI(Tl)	80	8000	400	50	21	4.41
HPGe	200	6000	400	100	21	0.19

Table 1: Trapezoidal filter parameters which optimize resolution (R) of the 1332keV peak.

4.2 Energy calibration

The energy calibration of the detectors has fundamental importance in properly identifying the different γ -transitions. In order to calibrate the two detectors, we recorded the spectrum emitted by two sources with well-known transition energies: ^{241}Am with a 59keV transition and ^{60}Co with 1173keV and 1332keV transitions.¹ In the case of the NaI(Tl) (because of the low

¹See www.nucleide.org/DDEP_WG/Nuclides/

threshold) we also saw the 26 keV transition of ^{241}Am and it was taken into account for the calibration. The peak energies have been deduced from the mean of a gaussian fit usually using as background a polynomial of the first order (in some cases to better reproduce the edge on the left side it has been used a step function). To obtain the calibration function the energies, expressed in arbitrary units, have been fitted to the nominal values: $E[\text{a.u.}] = p_0 + p_1 \cdot E[\text{keV}]$.

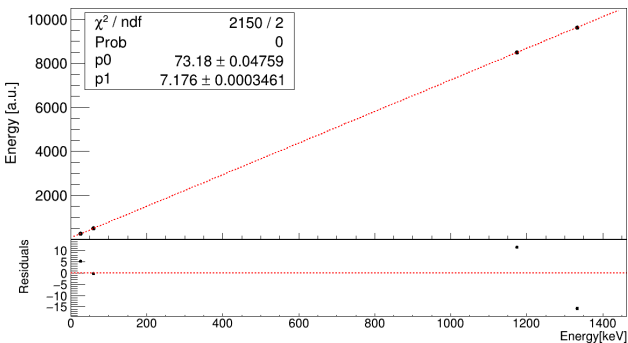


Figure 1: Calibration fit results for NaI(Tl).

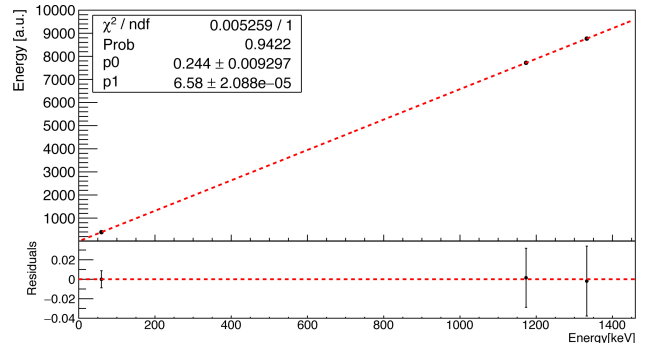


Figure 2: Calibration fit results for HPGe.

Detector	E_{26} [a.u.]	E_{59} [a.u.]	E_{1173} [a.u.]	E_{1332} [a.u.]	p0 [a.u.]	p1 [a.u./keV]
NaI(Tl)	269.4 ± 0.1	504.1 ± 0.2	8503.6 ± 0.5	9619.1 ± 0.6	73.18 ± 0.05	7.1756 ± 0.0003
HPGe	-	392.003 ± 0.001	7719.690 ± 0.003	8767.590 ± 0.004	0.244 ± 0.009	6.57966 ± 0.00002

Table 2: Energy calibration results. The 26 keV peak of ^{241}Am in the HPGe was not considered since it was only partially detected because of the high threshold.

5 Detector efficiency

In this experiment, a good estimation of the efficiency of the detectors is important, since it is necessary to correctly estimate the activity of the analyzed samples. The absolute efficiency (ϵ) of a full-energy peak is defined as the ratio between the number of photons of a γ transition recorded divided by those emitted by the source. It is a function of the peak energy and it depends on the intrinsic efficiency (ϵ_I) and the acceptance (ϵ_A) of the detector, through the relation:

$$\epsilon = \epsilon_I \cdot \epsilon_A \quad (1)$$

5.1 Intrinsic efficiency

The intrinsic efficiency of a full-energy peak is defined as the ratio between the number of photons of a γ transition recorded (N_{rec}) divided by those that hit the detector (N_{inc}). To estimate it we followed the next procedure:

- The sources of ^{241}Am and ^{60}Co have been placed at a known distance with respect to the detector used. For each detector, there is a specific position to place the source and to correctly estimate the acceptance (in Fig. 3 the position of the source is defined A for HPGe and B for NaI(Tl)).
- Each emission spectrum has been acquired for about 10 min.
- In the case of the HPGe detector it has been acquired also a spectrum of ^{152}Eu (placed in the same position of the other two sources) for about 30 min.

- It has been acquired a background spectrum (without sources) for about 30 min. Since in configuration B the source was out of the cockpit, in the case of NaI(Tl) the background has been taken with open cockpit (for the HPGe instead it was closed).

The net number of events recorded in a peak is estimated through the area of a gaussian fit (using a polynomial background) of the peak in the net spectrum (obtained by subtracting the background normalized to the acquisition time of the spectrum). From the source activity and the fraction of decays that produce a given γ transition² it is possible to estimate the number of photons emitted per unit of time by the source with a certain energy. In order to estimate the number of photons that hit the sample it is necessary to consider the acceptance of the detector which is $\epsilon_A = \frac{S_{det}}{D_{so}^2}$ (where S_{det} is the surface of the detector and D_{so} is its distance to the source).

The intrinsic efficiencies obtained from the HPGe has been fitted (as function of the photopeak energy E_γ expressed in keV) using the RADWARE funtion³:

$$\ln(\epsilon_I) = [(A+Bx+Cx^2)^{-G} + (D+Ey+Fy^2)^{-G}]^{-1/G} \quad (2)$$

where $x = \ln\left(\frac{100}{E_\gamma}\right)$, $y = \ln\left(\frac{1000}{E_\gamma}\right)$ and the others are fit parameters. This function (in Fig. 4) will be useful to determine the intrinsic efficiency of the detector for the γ -transitions of the samples (Sec. 6). The efficiency curve of the NaI(Tl) detector is more difficult to plot since there are only three points. We used a polynomial function given by⁴:

$$\epsilon_I = a + bE_\gamma + cE_\gamma^3 \quad (3)$$

where a, b and c are free parameters (the fit is shown in Fig. 5).

The distance of the sources with respect to HPGe was $D_{Det-A} = (20.5 \pm 0.5)cm$ and corresponds to an acceptance of $\epsilon_{A,HPGe} = 0.029 \pm 0.001$ (considering the nominal detection area $1200mm^2$).

The distance of the sources with respect to NaI(Tl) was $D_{Det-B} = (28.0 \pm 0.5)cm$ and corresponds to an acceptance of $\epsilon_{A,NaI} = 0.056 \pm 0.002$ (considering the nominal detection area $1200mm^2$).

We have observed that the intrinsic efficiency of the HPGe estimated using the nominal detection area of $1200mm^2$ has a peak around ~ 1.2 which is not possible. Since the relative efficiency (Fig. 6) is similar to what is expected we have supposed that there is a common factor that affects the total amplitude. A distance detector-source different from what we measured of 1 cm doesn't change radically the amplitude: moreover, the distance should be at most higher than the previous one (we took as the reference point for this measurement the surface of the endcap) so the efficiency should be higher. The activity can be at most lower than the reference one: also in this case the result is that the efficiency should be higher. In conclusion, the only parameter that we didn't measure directly and that can drastically affect the efficiency amplitude is the detection area. We didn't know exactly the model of the detector but we found in the documentation⁵

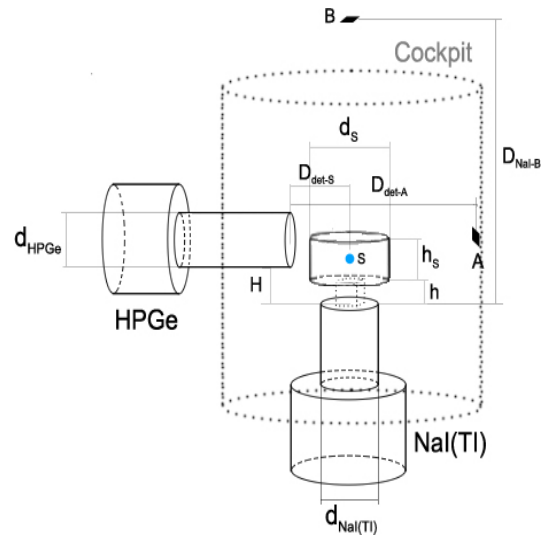


Figure 3: Detectors geometry.

²See www.nucleide.org/DDEP_WG/Nuclides/

³D. C. Radford, Nucl. Instr. and Meth. in Phys. Res. A 361, 297 (1995).

⁴A. Mouhti et al. "Validation of a NaI(Tl) and $LaBr_3(Ce)$ detector's models via measurements and Monte Carlo simulations", Journal of Radiation Research and Applied Sciences, 335-339 (2018).

⁵<https://www.ortec-online.com/-/media/ametekortec/brochures/gamma-x.pdf>

that almost all ORTEC HPGe detectors with endcap of diameter 70mm have a crystal diameter in the range of [50mm, 60mm]. We supposed that our crystal has a diameter of $(55 \pm 5)\text{mm}$ finding a detection area of $(2400 \pm 200)\text{mm}^2$. With this value we obtained a reliable result for the efficiency (black plot in Fig. 4): we kept this result for the following analysis. The results of the intrinsic efficiencies of both detectors⁶ are summarized in the Tab. 3-4.

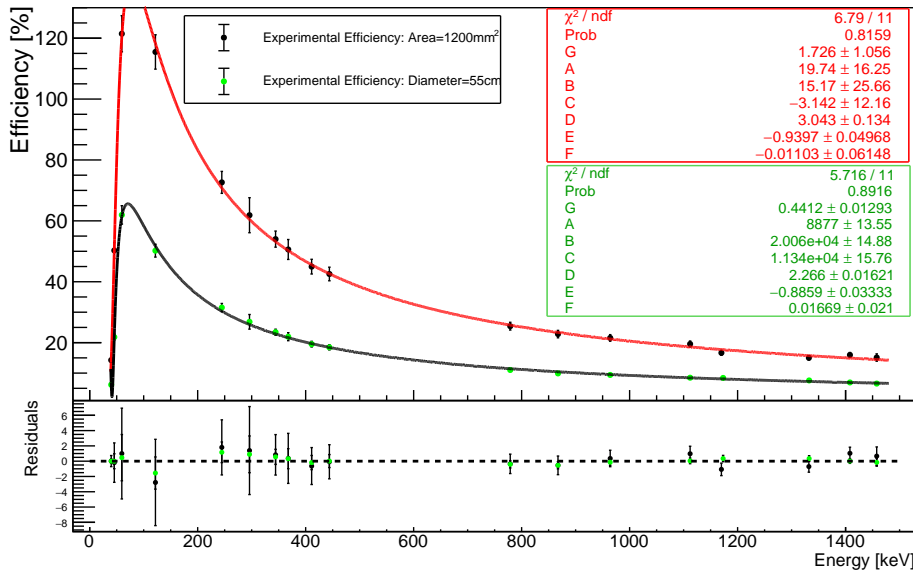


Figure 4: Intrinsic efficiencies of HPGe fitted using RADWARE function with effective detector surface of: 1200mm^3 (red) and 2400mm^2 (black).

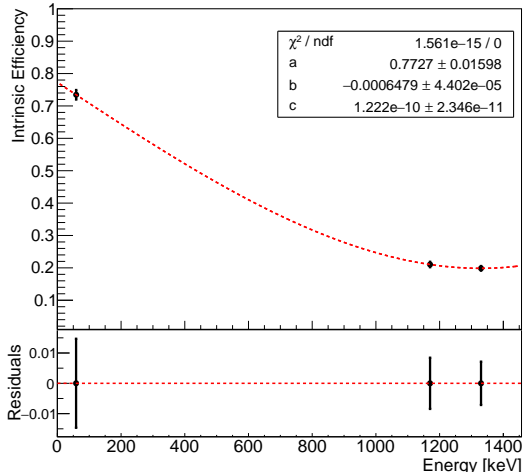


Figure 5: Intrinsic efficiency of NaI(Tl) fitted using the function given by Eq. 3.

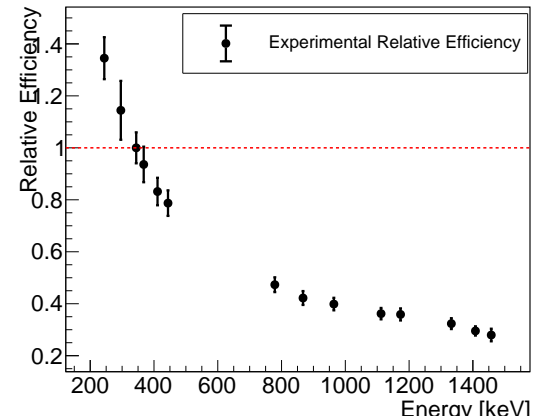


Figure 6: Relative efficiency of HPGe with respect to the transition at 344 keV.

Isotope	Energy [keV]	Intensity [%]	ϵ_I [%]
²⁴¹ Am	59.5	35.9	73.4 ± 1.5
⁶⁰ Co	1173.2	99.8	21.0 ± 0.8
⁶⁰ Co	1332.5	100.0	19.9 ± 0.7

Table 3: NaI(Tl) intrinsic efficiency results.

⁶The site where we found the information about the observed transition is <http://www.nucleide.org>

Isotope	Energy [keV]	Intensity [%]	ϵ_I [%]	Isotope	Energy [keV]	Intensity [%]	ϵ_I [%]
^{241}Am	59.5	35.7	53.6 ± 2.6	^{152}Eu	367.8	0.9	22.2 ± 1.4
^{60}Co	1173.2	99.8	7.3 ± 0.4	^{152}Eu	411.1	2.2	19.7 ± 1.1
^{60}Co	1332.5	100.0	6.6 ± 0.3	^{152}Eu	443.9	3.1	18.7 ± 1.0
^{152}Eu	39.9	59.1	6.3 ± 0.3	^{152}Eu	778.9	12.9	11.2 ± 0.6
^{152}Eu	45.6	14.9	22.1 ± 1.1	^{152}Eu	867.4	4.2	10.0 ± 0.5
^{152}Eu	121.8	28.4	50.7 ± 2.5	^{152}Eu	964.0	14.5	9.5 ± 0.5
^{152}Eu	244.7	7.6	31.9 ± 1.6	^{152}Eu	1112.1	13.6	8.6 ± 0.4
^{152}Eu	296.0	0.4	27.2 ± 2.5	^{152}Eu	1408.0	21.0	7.0 ± 0.3
^{152}Eu	344.3	26.6	23.7 ± 1.2	^{152}Eu	1457.6	0.5	6.6 ± 0.5

Table 4: HPGe intrinsic efficiency results with detection area of 2400mm^2 .

6 Measurement of sample activity

In this section, we will report the results obtained from the analysis of some organic and inorganic samples. The samples have different activities so the acquisition time (T_{acq}) can change in order to obtain a good statistic. Typically the acquisition time was about 20-30 min, except for water whose spectrum has been recorded for all the night using the NaI(Tl) detector. The spectra of the other samples have been recorded using both detectors.

We have measured the background of the two detectors for an acquisition time of about 30 min. In the case of water, since the long acquisition time significantly reduces statistical uncertainties, we have also recorded another background for all the night with NaI(Tl). For each sample, the background normalized to the acquisition time has been subtracted from the spectrum. This procedure allows to obtain a "net" spectrum. In this way, it is possible to find the γ -peaks emitted by the sample and, using a gaussian fit (add to a polynomial background), to count the number of events for each transition. Knowing the geometry of the samples (and so the solid angle with respect to the detector) and the intrinsic efficiency, as a function of the energy (Sec. 5.1), we can measure the activity of the radioactive isotopes that are present in the samples by summing the activities of all their identified transitions.

To estimate the solid angle and the relative error in the different configurations, we approximated each sample to a material point and we geometrically measured the distances of the center from the surfaces of the detectors. Each sample was placed on top of the NaI detector and in front of the HPGe detector (in some cases the sample has to be lifted by a thickness of polystyrene) (see Fig. 3). Given the small distance between the detector's surface and the sample, the solid angle was not approximated as the ratio between surface and distance squared, but it was calculated analytically based on the position of the samples. The error associated with this distance is estimated from the uncertainty of the effective position of the sample center. Assuming a normal distribution of the effective center, we get an uncertainty $\sigma_{sam} = 0.34 d_{sam}$ (where d_{sam} is the sample diameter). For both the HPGe detector and the NaI detector, we calculated the error of the solid angle by propagating the uncertainty associated with the distance from the center of the sample. Since the samples were positioned near the detectors, the uncertainties of the solid angles are large and they heavily affect the accuracy of the activity measurements.

6.1 Mushrooms of 1986

$T_{acq} = 36' 01''$	$m_{mush} = 15\text{g}$	$\Omega_{NaI} = (0.5 \pm 0.1)\text{sr}$	$\Omega_{HPGe} = (0.4 \pm 0.2)\text{sr}$
Isotope		Activity(NaI) [mBq/g]	Activity(HPGe) [mBq/g]
^{137}Cs		-	160 ± 50

Table 5: Activity estimated with NaI(Tl) and HPGe detectors of mushrooms.

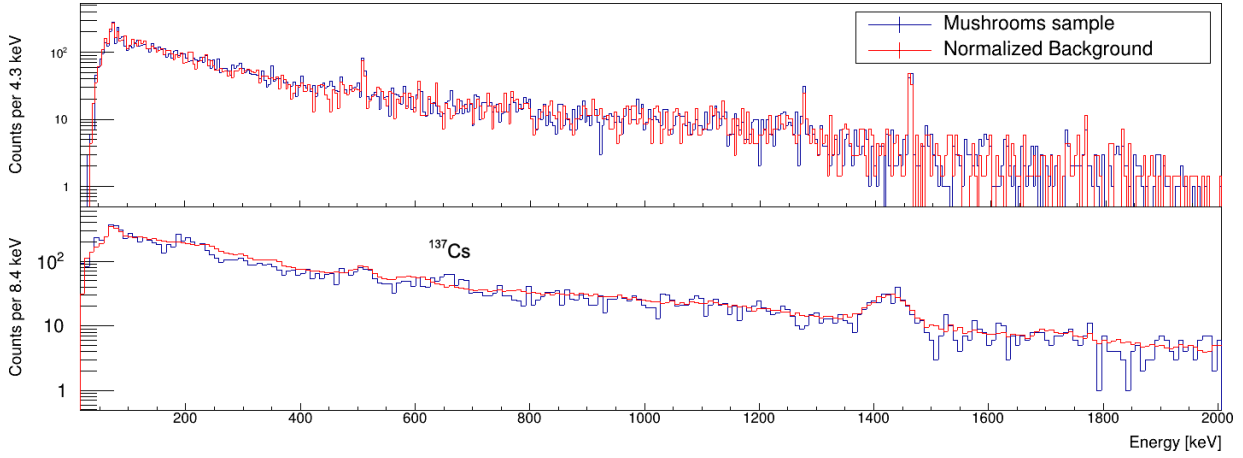


Figure 7: Spectra of mushrooms recorded by HPGe (top) and NaI(Tl) (bottom) with background. The spectrum recorded by HPGe has not a sufficient statistics to observe the cesium peak.

6.2 Water

$T_{acq} = 20h\ 12'\ 40''$	$m_{water} = 500g$	$\Omega_{NaI} = (1.5 \pm 0.3)sr$
Isotope	Activity(NaI) [mBq/g]	
^{137}Cs	9.18 ± 0.08	

Table 6: Activity estimated with NaI(Tl) detector of water.

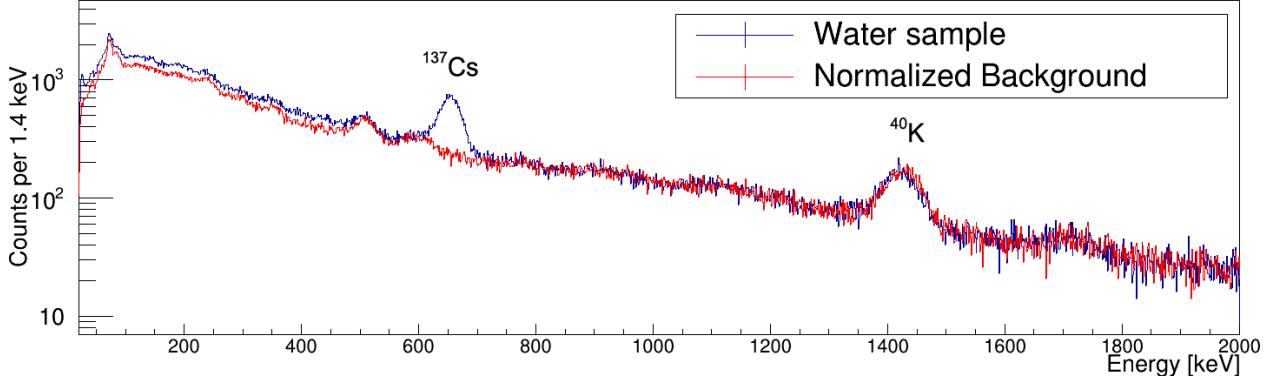


Figure 8: Spectrum of water recorded by NaI(Tl) with background.

6.3 Porphyry

$T_{acq} = 25'\ 12''$	$m_{porp} = 490g$	$\Omega_{NaI} = (1.7 \pm 0.3)sr$	$\Omega_{HPGe} = (0.5 \pm 0.2)sr$
Isotope	Activity(NaI) [mBq/g]	Activity(HPGe) [mBq/g]	
^{212}Pb	29 ± 1	7 ± 3	
^{214}Pb	17 ± 4	18 ± 5	
^{214}Bi	23 ± 5	5 ± 1	
^{228}Ac	-	5 ± 3	
^{208}Tl	-	4 ± 2	
^{40}K	80 ± 14	50 ± 20	

Table 7: Activities estimated with NaI(Tl) and HPGe detectors of porphyry.

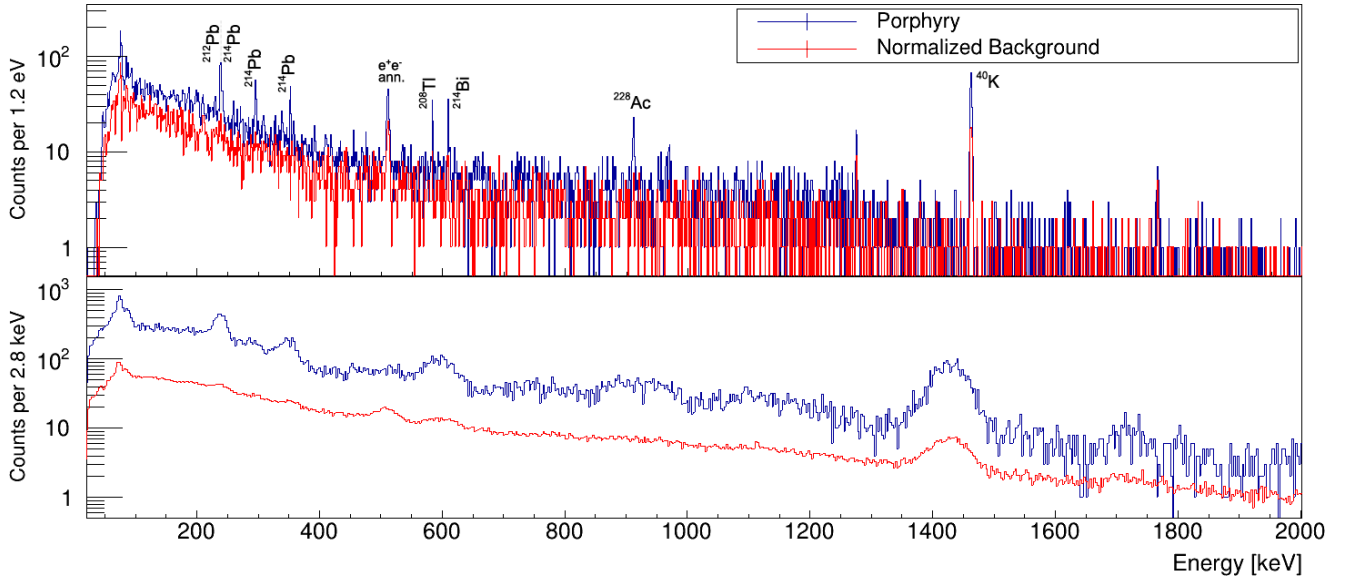


Figure 9: Spectra of porphyry recorded by HPGe (top) and NaI(Tl) (bottom) with background.

The resolution of NaI(Tl) detector is too low to distinguish all the spectral peaks as in the case of the HPGe. As a consequence we can measure with NaI(Tl) only part of the transitions. Moreover with that detector there is an higher component of background. For these reasons we proceeded with the analysis using only the HPGe detector.

6.4 Autunite

$T_{acq} = 25'$	$m_{aut} = 30g$	$\Omega_{HPGe} = (0.7 \pm 0.3)sr$
Isotope	Activity(HPGe) [mBq/g]	
²²⁶ Ra	740 ± 300	
²¹⁴ Pb	7600 ± 2000	
²¹⁴ Bi	10200 ± 3000	

Table 8: Activities estimated with HPGe detector of autunite.

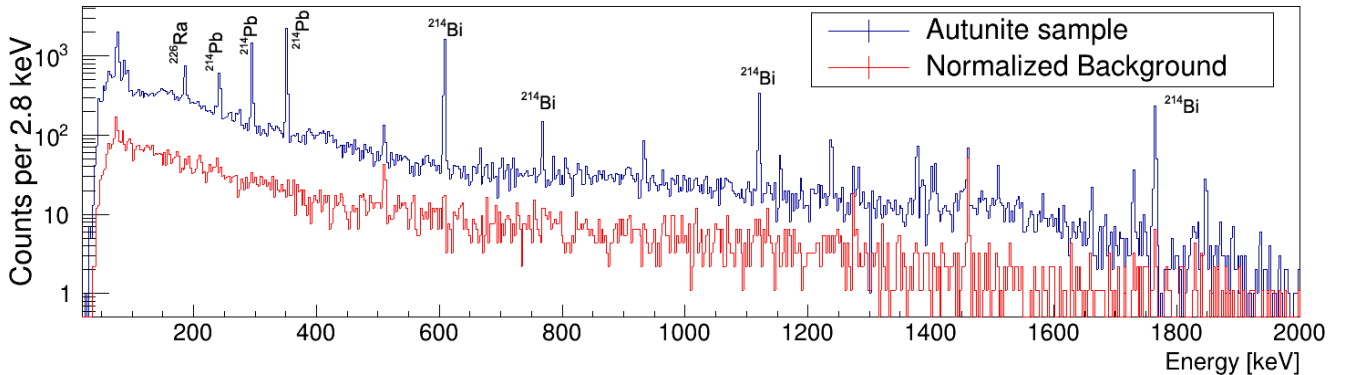


Figure 10: Spectra of autunite recorded by HPGe with background.

6.5 Zirconium oxide

$T_{acq} = 27'$	$m_{zirc} = 1870\text{g}$	$\Omega_{HPGe} = (0.4 \pm 0.2)\text{sr}$
Isotope	Activity(HPGe) [mBq/g]	
^{226}Ra		60 ± 30
^{214}Pb		720 ± 260
^{214}Bi		1900 ± 950
^{228}Ac		370 ± 200

Table 9: Activities estimated with HPGe detector of zirconium oxide.

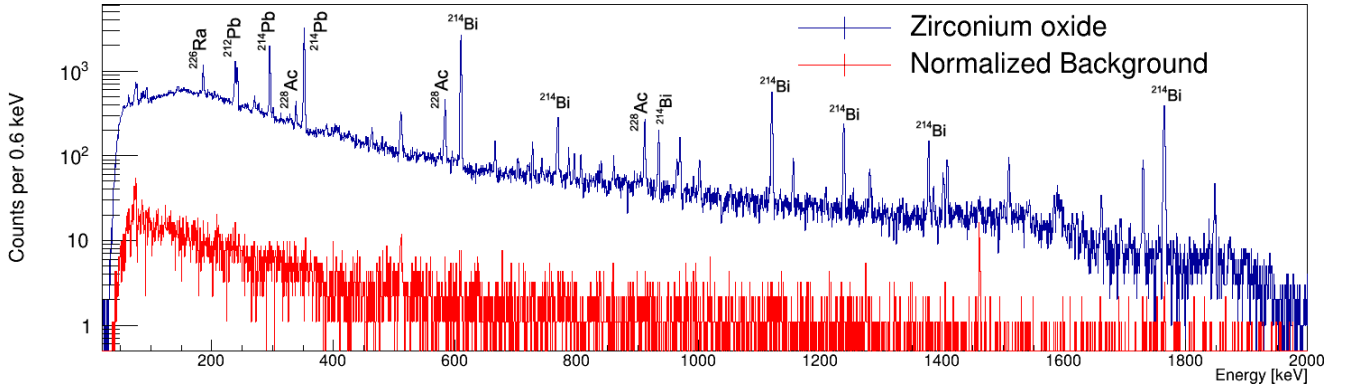


Figure 11: Spectrum of zirconium oxide recorded by HPGe with background.

7 Measurement of Radon activity

Let's proceed with the estimation of the radioactivity of the radon present in the lower floors of the Polo Didattico Department. To do this, a canister of activated charcoal, designed to absorb and filter the air that holds radon and its products, was left exposed in a closed room for the duration T_s of 5 consecutive days ($T_s = 7200\text{min}$). After that, the spectra of the exposed canister, a calibration canister (which contains the ^{226}Ra source with activity $A_{Ra} = 14.2\text{nCi}$) and an unexposed canister (used to measure the background) were analyzed: all the spectra have been recorded for the same acquisition time $T_{acq} = 30\text{min}$. Each canister has been placed inside the cockpit, on top of the NaI(Tl) scintillator. Following the EPA's standard, the radon's activity per liter of air, named RN, is given by:

$$RN = \frac{N \times A_{Ra}}{DF \times E \times CF \times T_s} \quad CF = CF(2) \times \frac{AF(T_s)}{AF(2)} \quad (4)$$

where N is the net number of events in the spectra inside an energy window that contains all the major γ transitions, DF is a decay factor that counts how much absorbed radon can decay during the collecting phase, so that we cannot count its radiation's emission, E is the net number of events of the calibration canister (considered in the same energy window and for the same acquisition time of the exposed canister) and CF is a calibration factor that estimates the amount of air (liter) per minutes that the canister can filter during the exposure time.

In Eq. 4 The factor CF is calculated starting from a $CF(2)$ of 2 days exposure time multiplied by some "adjusting factors" AF . These coefficients depend on the exposure time, the water gain due to the absorption of water vapor and the average humidity during the exposure. By measuring the weight increase of the exposed canister, we can estimate the water gain and the humidity. The weight has varied from an initial value $m_{can,i} = (152.3 \pm 0.1)\text{g}$ to a final value

$m_{can,f} = (163.9 \pm 0.1)g$, so the estimated water gain for an exposure of 48 hours turns out to be $G_{H_2O} \simeq 4.6g$. The average humidity for this water gain value is conventionally fixed as 80%. The coefficients result:

$$CF(2) = (0.105 \pm 0.005) \frac{l}{min} \quad AF(2) = (0.092 \pm 0.003) \frac{l}{min} \quad AF(T_s) = (0.037 \pm 0.002) \frac{l}{min} \quad (5)$$

The calibration factor (Eq. 4) is: $CF = (0.042 \pm 0.003) \frac{l}{min}$.

The decay factor DF depends exponentially on the exposure time and on the half-life of radon ($T_{1/2,Rn} = 5051\text{ min}$):

$$DF = e^{\frac{-\ln(2)T_s}{T_{1/2,Rn}}} = 0.61 \quad (6)$$

We want to compare the activity of the ^{222}Rn inside the canister with respect to a known source of ^{226}Ra . In order to do this, we can consider the principal common transitions of the two sources (which are inside the range of [200keV, 1200keV]) and divide the net number of events (obtained by subtracting the background) in this region of the canister exposed N by the number of events of the calibration canister E (Tab. 10).

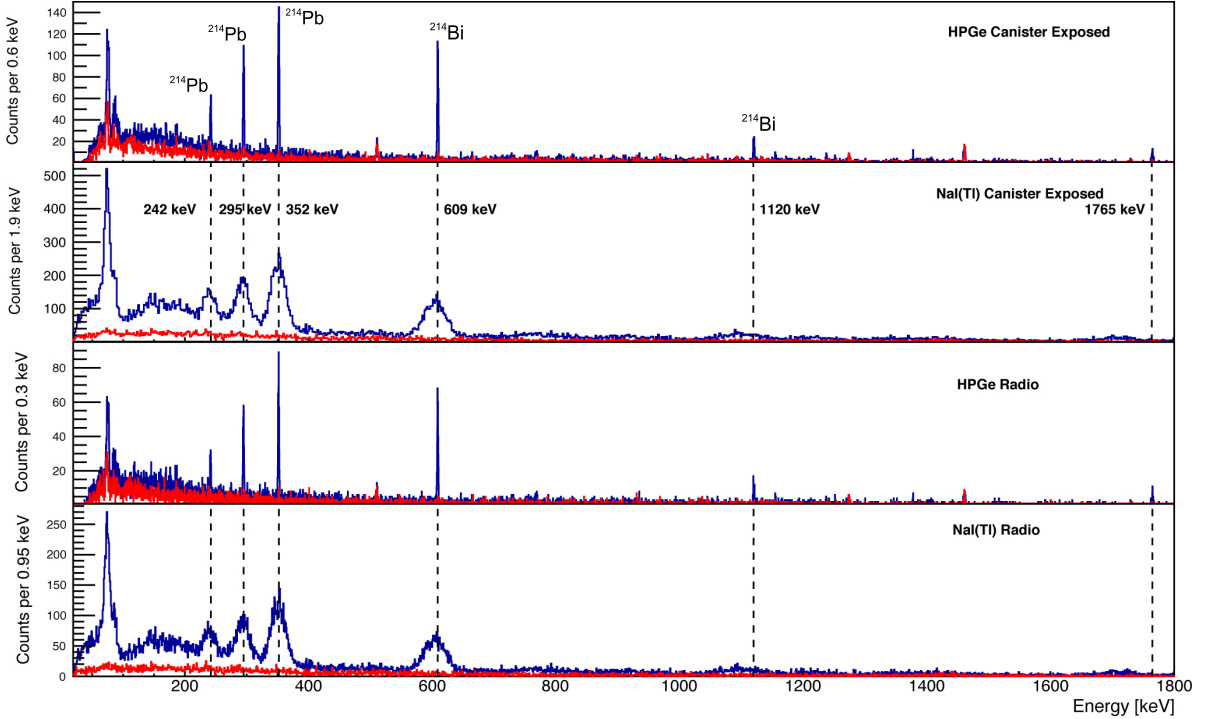


Figure 12: Spectra of the exposed canister and the calibration canister with HPGe and NaI(Tl) detectors (blue) overlapped to their backgrounds (red).

Detector	Range	$A_{tot,can}$	$A_{tot,Ra}$	A_{bkg}	N	E	N/E
HPGe	[230keV, 1130keV]	7630 ± 90	19800 ± 140	3810 ± 60	3820 ± 110	15980 ± 150	0.239 ± 0.007
NaI(Tl)	[200keV, 1200keV]	22080 ± 150	84300 ± 290	4880 ± 70	17200 ± 160	79420 ± 300	0.217 ± 0.002

Table 10: Results obtained by the analysis of the experimental spectra of exposed canister and calibration canister for both detectors: $T_{acq} = 30\text{min}$ for each spectrum.

An alternative way, which exploits the high resolution of the HPGe, consists in measuring the areas of the common peaks (in the spectrum with background subtracted) and plotting the number of counts measured in the canister exposed with respect to that measured in the calibration

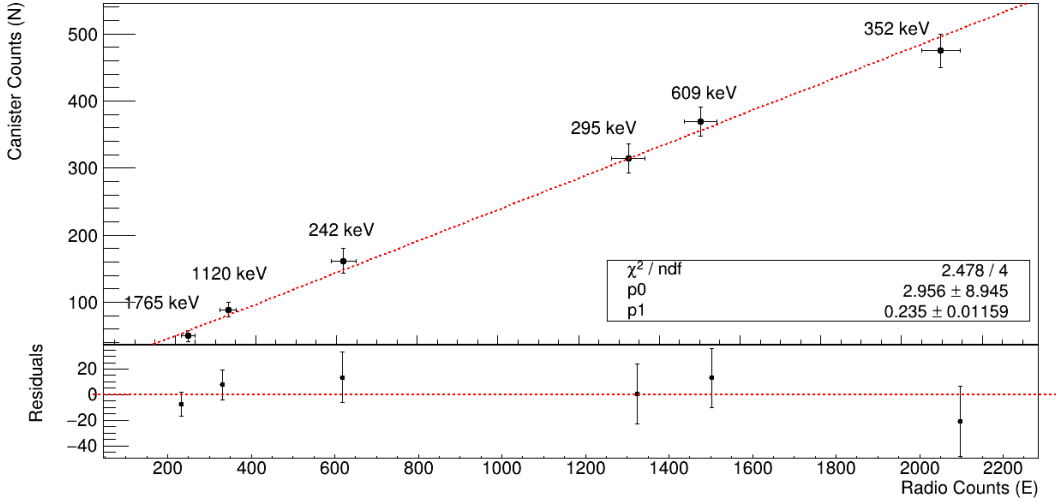


Figure 13: Linear fit that shows the correlation between the net number of events in the canister exposed and in the radium source under the some peak for HPGe.

canister (Fig. 13) using a linear fit. The ratio of the activities of the two samples is given by the angular coefficient: $N/E = 0.24 \pm 0.01$.

The uncertainties of N/E (in Tab. 10) estimated from the ratio of the areas in the same energy range consider the Poisson contributions of the spectra of canister/radium and that of the background. Although these results have lower statistical uncertainties with respect to that estimated using the linear fit there is a contribution of systematic error due to the not perfect subtraction of the background. For this reason, the best estimation of N/E is that obtained from the linear fit. Inserting this parameter in the Eq. 4 we can finally estimate the ^{222}Rn activity:

$$RN = (18 \pm 1) \frac{pCi}{l} = (650 \pm 50) \frac{Bq}{m^3} \quad (7)$$

8 Conclusions and perspectives

In this experiment we measured the activity of different samples and we noticed the presence, in many of them, of the decay products of ^{238}U (such as ^{214}Pb , ^{214}Bi and ^{226}Ra) and ^{232}Th (such as ^{228}Ac and ^{212}Pb). We also found in the rocks traces of ^{40}K which is a typical radioactive isotope commonly present in the environment (for example in the wall): for this reason, it was also present in the background spectra. From the analysis of water and mushrooms, we observed small traces of ^{137}Cs which is a typical product of artificial nuclear fission. Its activity is low, so we didn't obtain an accurate estimation of it in the mushroom sample: it is suggested to acquire its spectrum for all night as it was done for the water.

In this work has been obtained also an estimation of ^{222}Rn activity in the cellar of Polo Didattico: $RN = (650 \pm 50) Bq/m^3$. This value is greater than the maximum value permitted by the directive 2013/59/Euratom which establishes a maximum activity of $300 Bq/m^3$ in a workplace. The activity that we estimated is probably affected by some systematic errors due to the not perfect estimation of the correction factors (they strictly depend on the environmental condition such as the humidity and so they are difficult to be accurately evaluated).

Eventually, we observed the differences in the results that can be obtained using the NaI(Tl) and HPGe detectors. The NaI(Tl) has typically a higher efficiency that has been used to estimate the activity of ^{137}Cs but a low resolution, so it is difficult to identify many isotopes. The HPGe instead has a high resolution, which was exploited to find many isotopes, but lower efficiency: it is useful when there are many transitions but it requires longer acquisition times.